

S. Boedo and J.F. Booker,

"Finite element analysis of elastic engine bearing lubrication: Application",
Traitement des Problèmes de Lubrification par la Méthode des Eléments Finis,
Revue Européenne des Eléments Finis, Vol. 10, No. 6-7/2001, pp 725-739.

Finite Element Analysis of Elastic Engine Bearing Lubrication: Application

S. Boedo* — J.F. Booker**

**Department of Mechanical Engineering
Rochester Institute of Technology
76 Lomb Memorial Drive, Rochester, NY 14623 USA
sxbeme@rit.edu*

*** Sibley School of Mechanical and Aerospace Engineering
Cornell University
Upson Hall, Hoy Road, Ithaca, NY 14853 USA
j.f.booker@cornell.edu*

ABSTRACT: This paper describes an application of finite element mode-based elastohydrodynamic lubrication analysis (as described in a companion paper) to the bearing and structural design of a dynamically loaded automotive connecting rod. Particular emphasis is placed upon description of the modeling process and upon computation of distributed stresses in the connecting rod. It is found that truncated model representations are adequate for computation of bearing performance (film thickness, film pressure) and structural performance (von Mises stress).

RÉSUMÉ: Cet article présente une application orientée vers le dimensionnement des paliers de bielle des moteurs thermiques d'automobile. Elle s'appuie sur l'analyse par la méthode des éléments finis de la lubrification élastohydrodynamique basée sur la méthode modale telle qu'elle est décrite dans un article associé. Un soin particulier est porté à la description des processus de modélisation et de calcul des contraintes agissant dans la bielle. Il est montré que des représentations sur une base modale tronquée sont bien appropriées pour le calcul des performances du palier (épaisseur du film, champ de pression) et de la sollicitation des structures (contrainte de Von Mises).

KEY WORDS: connecting rod, bearings, lubrication, stress, finite elements, elasticity, design

MOTS-CLÉS: bielle, palier, lubrification, contrainte, éléments finis, élasticité, dimensionnement

1. Introduction

Automotive big-end connecting rod bearings are subjected to periodic variations in relative surface motion and external loads, and hence, they provide excellent case studies to illustrate key features of transient elastohydrodynamic lubrication (EHL) algorithms. The elastic characteristics of the connecting rod are represented by either compliance or stiffness matrices typically obtained by static condensation of representative finite element models of various complexity. Early studies with transient EHL employed connecting rod models represented by two-dimensional plane stress finite elements [FAN 83] that were computationally fast but structurally inadequate. Some of the first realistic finite element connecting rod models employed three-dimensional isoparametric elements to capture basic structural details such as ribs, bolt supports and out-of-plane sleeve flexibility [OH 85], and corresponding EHL results showed that these three-dimensional features were important in properly assessing bearing performance.

The main dilemma facing the engine designer today is the choice of an appropriate model and computational strategy to apply to connecting rods. Extended formulations of transient EHL models applied to connecting rod bearings have included higher-order elements [MCI 89], mode shapes [KUM 90], mass-conservation [BOE 95], body forces [BON 95, BOE 97], vibration effects [KNO 96], and thermal effects [KIM 01], all of which have employed three-dimensional connecting rod models. Moreover, these studies typically represented the actual connecting rod with models truncated at arbitrary points along the connecting rod, with the thought that the key features of bearing deformation would be confined to the big-end crankpin portion. Furthermore, these studies only investigated the effect of connecting rod structure as it related to the lubricant response of the bearing, such as minimum film thickness, oil flow, and maximum film pressure.

The purpose of this paper is to evaluate how various lubrication models and connecting rod structural representations influence bearing performance and stress distributions in an actual production-level connecting rod. The mode-based elastohydrodynamic formulation [BOE 97, BOO 01] is employed in this study, assuming journal rigidity, smooth bearing surfaces, body forces arising from structural inertia, and a mass-conserving lubrication model.

2. Problem Formulation

Figure 1 shows complete and (radically) truncated *half-model* finite element representations, respectively, of a production-level connecting rod. Each model is constructed from 10-node isoparametric tetrahedral elements using ANSYS. In the complete half-model finite element representation, the bearing deformation on the small end bearing surface is restrained from radial deflection, and one node on the same surface is restrained from tangential deflection to prevent rigid body motion.

The truncated representation is completely restrained along the truncation plane. In both models, an X,Y,Z system frame is attached to the sleeve center, and the half-model assumption requires symmetry displacement boundary conditions invoked along the plane $Z = 0$. Structural specifications are provided in Table 1.

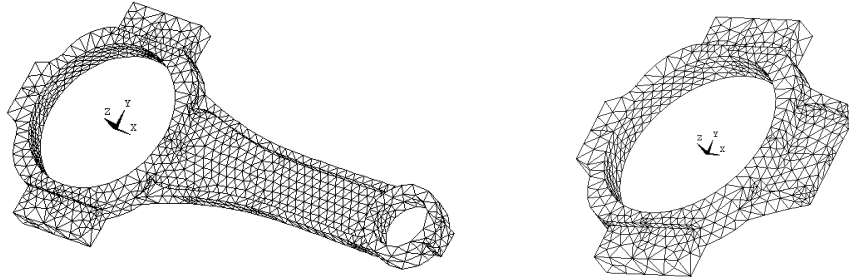


Figure 1. Complete and truncated half-model finite element connecting rod models

Computation of bearing duty (loads and kinematics) for the big-end connecting rod bearing are based on consideration of a composite crankshaft-connecting rod-piston rigid body mechanism connected with and supported by zero-clearance pin-jointed bearings as shown in Figure 2. The X', Y', Z' (inertial) block coordinate frame is fixed to the rigid engine block and its origin is situated at the crank main bearing. The cylinder axis lies along the X' axis, and all motion takes place in the $Z' = 0$ plane. The crankshaft rotates at a constant angular velocity $\omega = d\theta/dt$ about the Z' axis.

For convenience, the actual connecting rod with center-to-center length L , mass M , center of mass \bar{x} , and polar moment of inertia J (about the X,Y,Z origin) is replaced by a dynamically equivalent model comprised of big and small end point masses M_b , and M_s , respectively, and a massless residual inertia J_r [PAU 79] as shown in Figure 2. In order that the actual and equivalent models have identical centers of mass, total mass, and polar moment of inertia, it follows that [BOE 89]

$$M_s = M\bar{x}/L \quad [1]$$

$$M_b = M(1 - \bar{x}/L) \quad [2]$$

$$J_r = J - M\bar{x}L \quad [3]$$

Table 1 *Dimensional specifications**(a) Connecting rod model specifications*

Young's modulus		210	GPa
Poisson's ratio		0.3	
structural density		7900	kg/m ³
connecting rod length	L	145	mm (center-to-center)
mass	M	0.2558	kg (half-model)
center of mass	\bar{x}	37.257	mm
polar moment of inertia	J	1.323×10^{-3}	kg-m ² (half-model)
small end mass	M _s	0.0657	kg (half-model)
big end mass	M _b	0.1901	kg (half-model)
residual inertia	J _r	-5.862×10^{-5}	kg-m ² (half-model)

(b) Bearing specifications

bearing diameter		60	mm
bearing length		10	mm (half-model)
radial clearance		20	μm
groove width		1	mm (half-model)
surface roughness		0	μm
liquid viscosity		7	mPa-s
liquid density		850	kg/m ³
supply pressure		400	kPa (gage)
ambient pressure		0	kPa (gage)
cavitation pressure		0	kPa (gage)

(c) Engine specifications

piston mass	M _{pist}	0.250	kg (half-model)
crank radius	R	42.5	mm
cylinder area	A _{cyl}	1290	mm ² (half-model)
crankshaft speed	ω	4000	rev/min

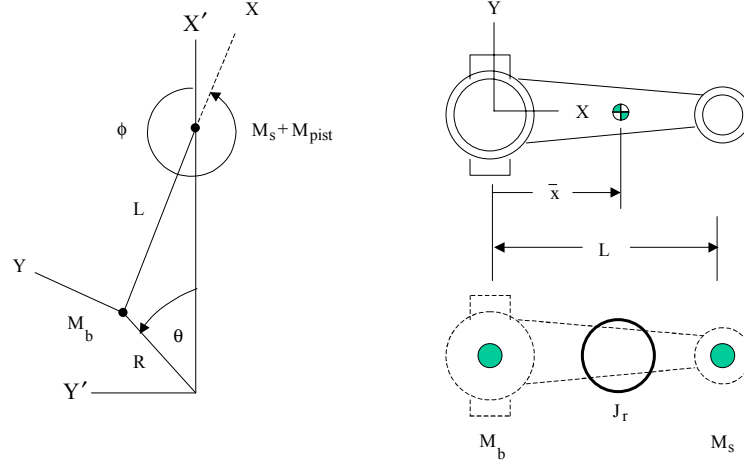


Figure 2. Engine mechanism and connecting rod approximation

Further assuming that the piston and small end masses are constrained to reciprocate along the X' axis, the external load transmitted from the journal to the big-end sleeve has block-frame components¹ [BOE 95]

$$F^{X'} = P_{\text{cyl}} A_{\text{cyl}} - M_b R \omega^2 \cos \theta - (M_s + M_{\text{pist}})(R \omega^2 \cos \theta + L \dot{\phi}^2 \cos \phi + L \ddot{\phi} \sin \phi) \quad [4]$$

$$F^{Y'} = -M_b R \omega^2 \sin \theta + (M_b R \omega^2 \cos \theta + F^{X'}) \tan \phi - J_r \ddot{\phi} / (L \cos \phi) \quad [5]$$

where P_{cyl} and A_{cyl} refer to cylinder pressure and cylinder cross-sectional area, respectively. The block frame load components are subsequently transformed into desired X, Y frame components by

$$F^X = +F^{X'} \cos \phi + F^{Y'} \sin \phi \quad [6]$$

$$F^Y = -F^{X'} \sin \phi + F^{Y'} \cos \phi \quad [7]$$

¹ Extended formulations to include gravity contributions and crankshaft acceleration are available elsewhere [BOE 89].

Figure 3 shows periodic time histories of *half-model* external load components in the system X,Y,Z frame based on engine specifications in Table 1 and cylinder pressure history given in Figure 4. It is interesting to observe that exact specification of point masses and residual ring inertia via equations [1-3] is not necessary for this connecting rod. Essentially identical results (not shown) are obtained by setting the residual inertia term to zero, thus only enforcing center of mass and total mass equivalence. Essentially identical results (not shown) are also obtained by approximating the connecting rod with big-end and small-end point masses of $2M/3$ and $M/3$, respectively, thus only enforcing total mass equivalence.

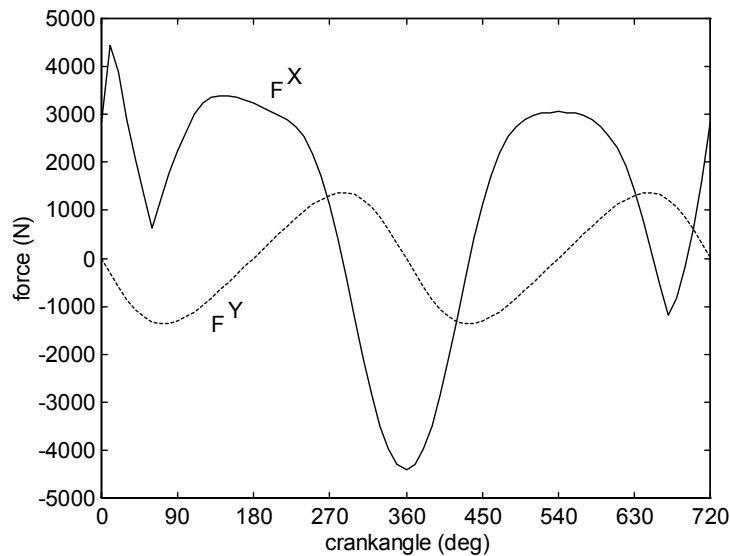


Figure 3. External load at 4000 rev/min

Figure 5 shows the first eleven members of a set of (unwrapped) mesh-invariant mode shapes corresponding to the relative stiffness matrix of the complete finite element model. Modes 1 and 2 exactly represent rigid-body journal translation while the others represent elastic deformation. Eigenvalues corresponding to these mode shapes are provided in Table 2. Essentially identical mode shapes (not shown) with similar eigenvalues (listed in Table 2) are obtained with the truncated model, suggesting that the rod stem immediately beyond the truncation plane is relatively rigid compared with the big-end region. In both models, eigenvalue magnitudes increase rapidly with mode number, suggesting that only a small set of modes would be required for subsequent analyses.

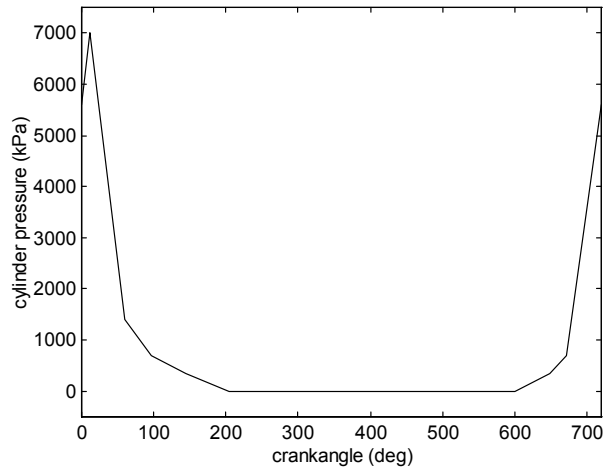


Figure 4. Cylinder pressure history at 4000 rev/min

Table 2. Mesh-invariant eigenvalues

Mode	Eigenvalue (TN/m ³)	
	Complete model	Truncated model
1	0	0
2	0	0
3	0.056	0.056
4	0.118	0.120
5	0.501	0.501
6	0.634	0.653
7	1.285	1.291
8	1.511	1.514
9	2.093	2.129
10	3.357	3.405
11	3.772	3.778

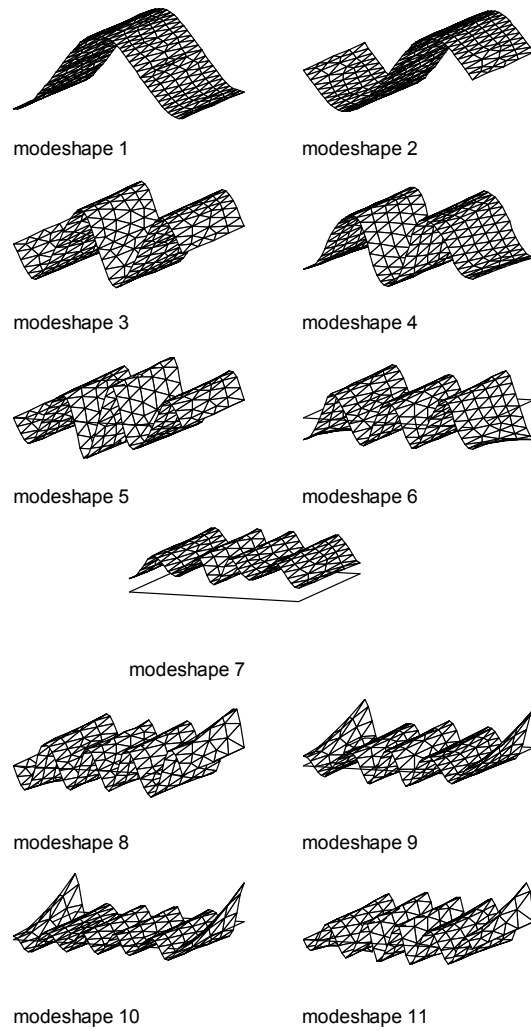


Figure 5. *Eigenvector mode shapes for complete finite element half-model (plane of symmetry towards observer)*

The lubricant film is represented by a uniform finite element mesh comprised of 3-noded fluid-film elements [BOO 72] divided into 72 elements along the circumferential direction and 10 segments in the axial direction. Fixed ambient pressure and liquid density boundary conditions are invoked along the bearing ends, while fixed supply pressure and liquid density boundary conditions are invoked on a circumferential groove along the bearing midplane. Fluid film specifications are provided in Table 1.

Note that the fluid film mesh and the sleeve surface mesh need not be identical, as nodal film thickness and nodal film rates are determined by mapping structure-based mode shapes onto the fluid film mesh [BOE 97]. This particularly attractive feature of the mode-based method allows wide flexibility in modeling the structural model while allowing for a separate fluid film model to account for special grooving arrangements or moving feed holes.

Each simulation is started with specified initial modal displacements and initial liquid nodal densities representing the set of state variables for modal EHL [BOE 97]. The simulation is run until periodicity over the duty cycle is attained, which for the case studies reported here, requires two complete engine cycles.

3. Results

Figure 6 shows the effect of body force contributions on periodic time histories of minimum film thickness and maximum film pressure obtained at 4000 rev/min for the complete connecting rod model. The number m represents modes 1 through m in Figure 5 selected prior to each simulation run. Regardless of whether or not body forces were included, it was found that 9 modes were adequate to capture the essential features of bearing deformation and film pressure histories. Solution comparisons indicate that body forces substantially enhance film thickness and substantially reduce film pressure, particularly when the load is in the cap region (270 to 450 degrees crankangle) and during rapid load reversal into the stem region at the onset of engine firing (660 degrees crankangle). These results are consistent with previous trends obtained with node-based calculations [BON 96] and with mode-based connecting rod models fed through a single crankpin hole [BOE 97].

Figure 7 shows the effect of cavitation algorithm on predicted bearing performance for the complete connecting rod model. Again, 9 modes were sufficient for both mass-conserving and quasi-static cavitation algorithms. It is observed that bearing performance trends are generally consistent with either cavitation algorithm over most of the engine cycle, with the main exception when the load is in the cap region (270 to 450 degrees crankangle). Here, the quasi-static cavitation algorithm predicts substantially thicker films and substantially lower pressures when compared with the mass conserving cavitation algorithm. These discrepancies in film thickness and film pressure trends between the quasi-static and mass-conserving cavitation algorithms are similar to EHL calculations conducted

with hole fed connecting rod bearings [BOE 95] but much greater than those obtained for a fully grooved *rigid* main bearing [JON 82]. It thus appears that elasticity and mass conservation may play a coupled role in connecting rod bearing performance.

Figure 8 shows that the results obtained from truncated and complete connecting rod models produce very similar trends in bearing performance, which would be expected as their corresponding mode shapes and mode eigenvalues are similar as well. As with the complete model, 9 modes were also found to be sufficient for the truncated model.

Figure 9 compares von Mises stress distributions in the complete and truncated models at an engine crankangle of 373 degrees, showing them to quite similar almost to the truncation plane. Similar results were observed at other crankangles. Note that these stresses arise from *both* induced surface film pressures and distributed body forces.

4. Summary

This paper has extended previous EHL analyses directed particularly at the design of connecting rods for automotive and off-highway applications. A mode-based EHL formulation as described in [BOE 97] and in the companion paper [BOO 01] is applied to a production-level connecting rod. As with previous applications, the lowest-order set of mode shapes obtained with this connecting rod has significant spatial variation in the axial direction, which discourages the use of two dimensional (plane stress/strain) model representations. Computational results indicate that body forces and mass-conserving cavitation are the two key factors that influence bearing performance (film thickness, film pressure) and structural performance (von Mises stress). The use of a truncated connecting rod model does not appear to alter the overall *relative* stiffness characteristics of the connecting rod. The results also lend confidence to previous published EHL studies that couple body force and elastic contributions.

5. Acknowledgement

This research used the facilities of the Mechanical Engineering PC Lab, Rochester Institute of Technology, Rochester, NY.

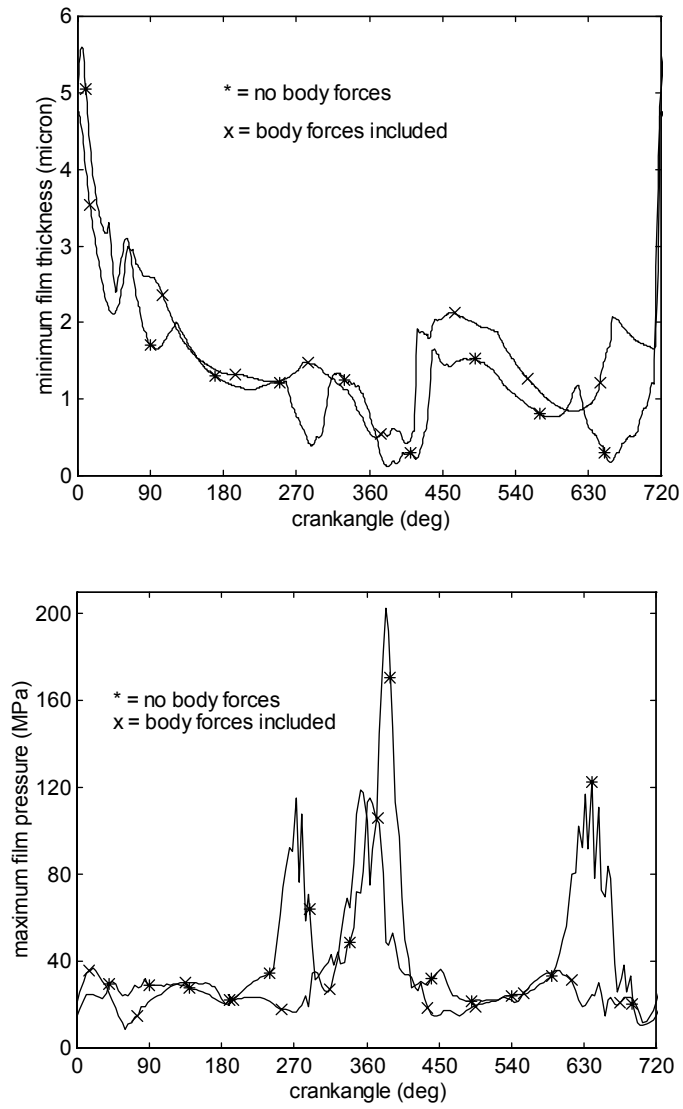


Figure 6. Comparison of bearing performance: complete model, $m = 9$, mass-conserving cavitation

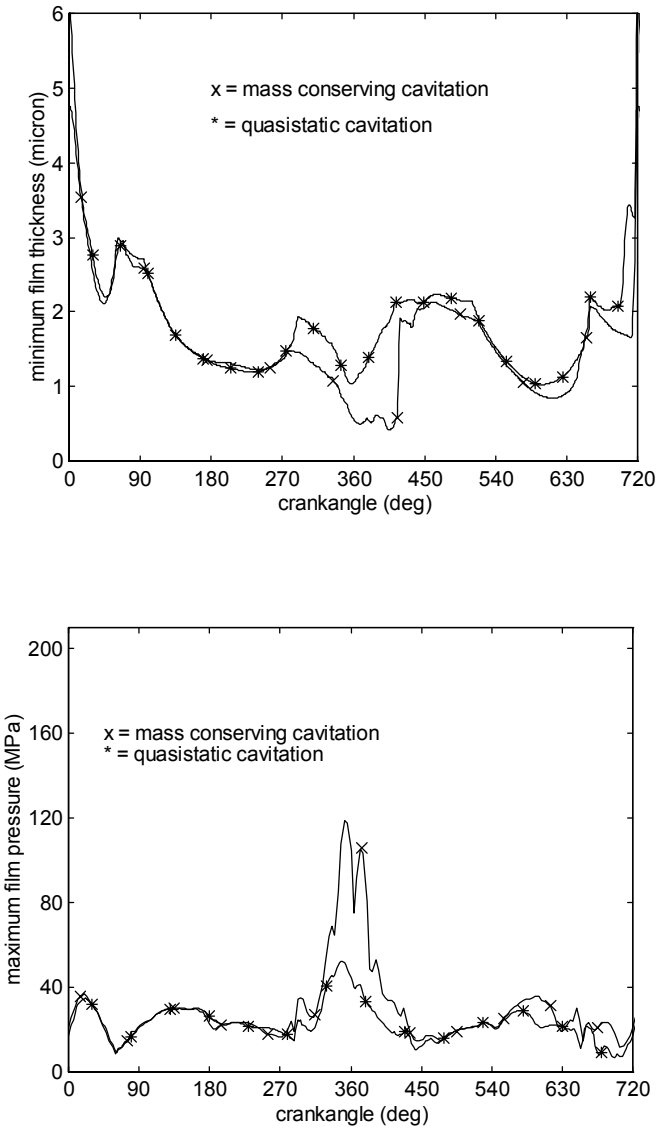


Figure 7. Comparison of bearing performance: complete model, $m = 9$, body forces included

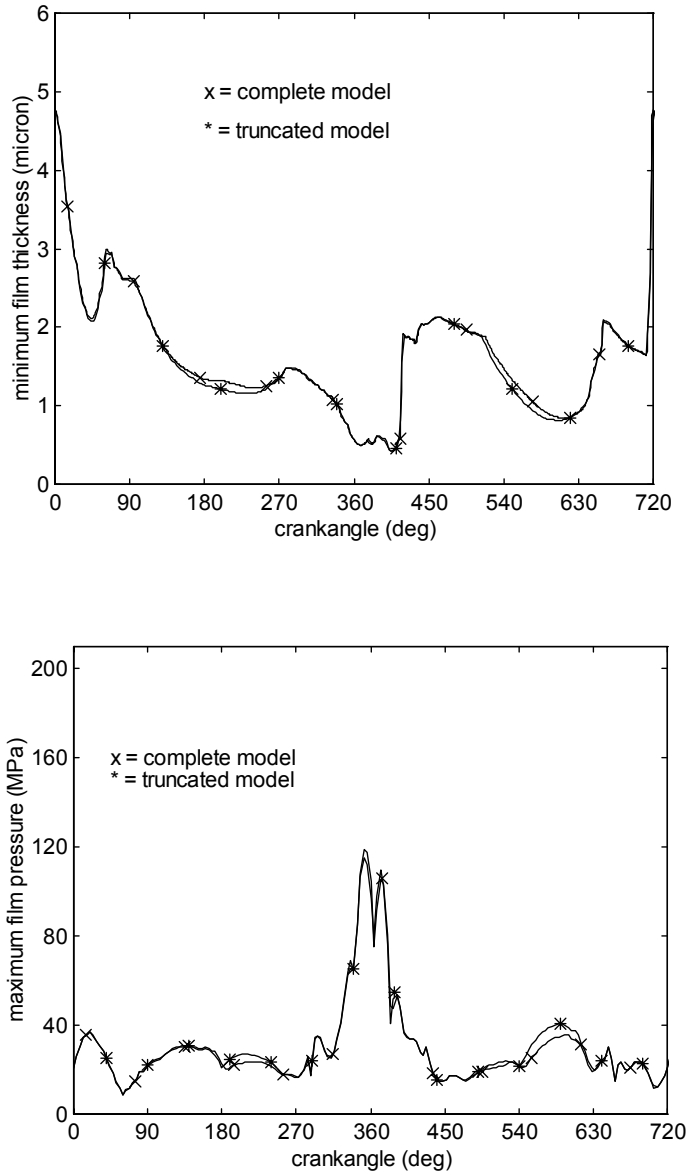


Figure 8. Comparison of bearing performance: body forces included, $m = 9$, mass-conserving cavitation

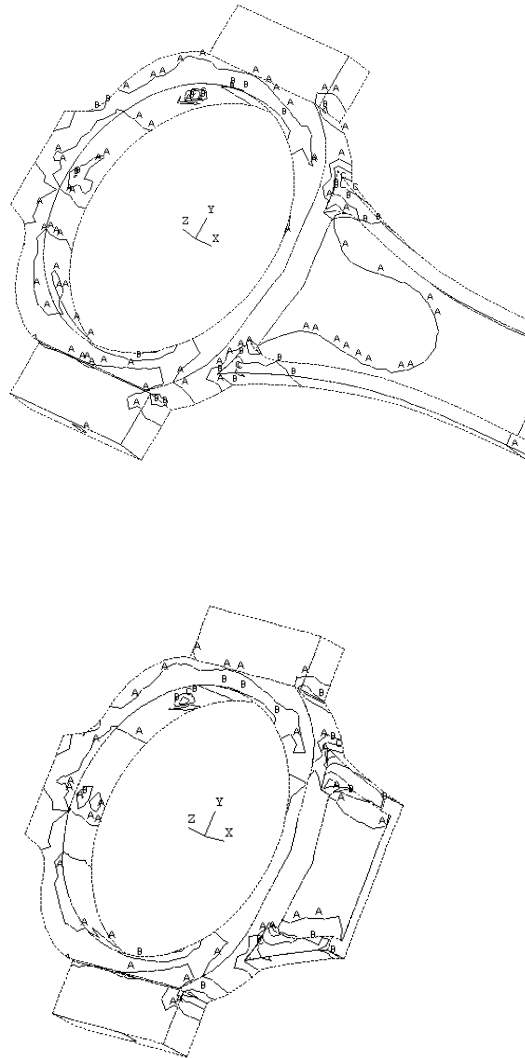


Figure 9. Von Mises stress distributions the complete and truncated connecting rod models at 373 degree crankangle ($A = 29$ MPa, $B = 58$ MPa, $C = 87$ MPa)

6. References

- [BOE 89] BOEDO S., BOOKER J.F., "Transient dynamics of engine bearing systems", *Proc. 15th Leeds-Lyon Symposium on Tribology, Tribological design of machine elements*, 1989, Elsevier, p. 323-332.
- [BOE 95] BOEDO S., BOOKER J.F., WILKIE M.J., "A mass conserving modal analysis for elastohydrodynamic lubrication", *Proc. 21st Leeds-Lyon Symposium on Tribology, Lubricants and Lubrication*, 1995, Elsevier, p. 513-523.
- [BOE 97] BOEDO S., BOOKER J.F., "Surface roughness and structural inertia in a mode-based mass-conserving elastohydrodynamic lubrication model", *ASME Journal of Tribology*, vol. 119, 1997, p. 449-455.
- [BON 95] BONNEAU D., GUINES D., FRÈNE J., TOPLOSKY J., "EHD analysis, including structural inertia effects and a mass conserving cavitation model", *ASME Journal of Tribology*, vol. 117, 1995, p. 540-547.
- [BOO 01] BOOKER J.F., BOEDO S., "Finite element analysis of elastic engine bearing lubrication: Theory", *Revue européenne des éléments finis (REEF)*, 2001, in press.
- [BOO 72] BOOKER J.F., HUEBNER K.H., "Application of finite elements to lubrication: An engineering approach", *ASME Journal of Lubrication Technology*, vol. 94, 1972, p. 313. Errata: vol. 98, 1976, p. 39.
- [FAN 83] FANTINO B., GODET M., FRÈNE J., "Dynamic behavior of an elastic connecting rod bearing--Theoretical study", *Studies of Engine Bearings and Lubrication, SAE SP-539*, 1983, p. 23-32.
- [JON 82] JONES G.J., LEE C.S., MARTIN F.A., "Crankshaft bearings: advances in predictive techniques incorporating the effects of oil holes and grooving", *AE Symposium, April 18-21, 1982, Paper LB 468/82*.
- [KIM 01] KIM B.-J., KIM K.-W., "Thermo-elastohydrodynamic analysis of connecting rod bearing in internal combustion engine", *ASME Journal of Tribology*, vol. 123, 2001, p. 444-454.
- [KNO 96] KNOLL G., LANG J., REINÄCKER A., "Transient EHD connecting rod analysis: Full dynamic versus quasi-static deformation", *ASME Journal of Tribology*, vol. 118, 1996, p. 349-355.
- [KUM 90] KUMAR A., GOENKA P.K., BOOKER J.F., "Modal analysis of elastohydrodynamic lubrication: A connecting rod application," *ASME Journal of Tribology*, vol. 12, 1990, p. 524-534.
- [MCI 89] MCIIVOR J.D.C., FENNER D.N., "Finite element analysis of dynamically loaded flexible journal bearings: A fast Newton-Raphson method", *ASME Journal of Tribology*, vol. 111, 1989, p. 597-604.
- [OH 85] OH K.P., GOENKA P.K., "The elastohydrodynamic solution of journal bearings under dynamic loading", *ASME Journal of Tribology*, vol. 107, 1985, p. 389-395.
- [PAU 79] PAUL B., *Kinematics and dynamics of planar machinery*, 1979, Prentice-Hall.